High duty factor plasma generator for CERN's Superconducting Proton Linac[a)]

J. Lettry,[1,b)] M. Kronberger,[1] R. Scrivens,[1] E. Chaudet,[1] D. Faircloth,[2] G. Favre,[1] J.-M. Geisser,[1] D. Küchler,[1] S. Mathot,[1] O. Midttun,[1] M. Paoluzzi,[1] C. Schmitzer,[1] and D. Steyaert[1]
[1]*CERN, CH1211 Geneva, Switzerland*
[2]*Rutherford Appleton Laboratory, Chilton, Didcot OX11 0QX, United Kingdom*

(Presented 22 September 2009; received 24 September 2009; accepted 30 November 2009; published online 24 February 2010)

CERN's Linac4 is a 160 MeV linear accelerator currently under construction. It will inject negatively charged hydrogen ions into CERN's PS-Booster. Its ion source is a noncesiated rf driven H^- volume source directly inspired from the one of DESY and is aimed to deliver pulses of 80 mA of H^- during 0.4 ms at a 2 Hz repetition rate. The Superconducting Proton Linac (SPL) project is part of the luminosity upgrade of the Large Hadron Collider. It consists of an extension of Linac4 up to 5 GeV and is foreseen to deliver protons to a future 50 GeV synchrotron (PS2). For the SPL high power option (HP-SPL), the ion source would deliver pulses of 80 mA of H^- during 1.2 ms and operate at a 50 Hz repetition rate. This significant upgrade motivates the design of the new water cooled plasma generator presented in this paper. Its engineering is based on the results of a finite element thermal study of the Linac4 H^- plasma generator that identified critical components and thermal barriers. A cooling system is proposed which achieves the required heat dissipation and maintains the original functionality. Materials with higher thermal conductivity are selected and, wherever possible, thermal barriers resulting from low pressure contacts are removed by brazing metals on insulators. The AlN plasma chamber cooling circuit is inspired from the approach chosen for the cesiated high duty factor rf H^- source operating at SNS. © *2010 American Institute of Physics.* [doi:10.1063/1.3277188]

I. H^- ION SOURCE FOR THE SPL PROJECT

Two types of high duty factor pulsed H^- ion sources for accelerators are currently operated at ISIS (Rutherford, 50 Hz) and SNS (Oak Ridge, 60 Hz). Both systems rely on Cs injection to produce H^- ions. A Cs-free H^- ion source[1] was developed at DESY and operated at the HERA accelerator up to 6 Hz repetition rate. This ion source was selected for CERN's Linac4[2,3] currently under construction. In CERN's Superconducting Proton Linac (SPL) project,[4] a major extension of Linac4 is proposed that would increase its energy from 160 MeV to 5 GeV and its repetition rate from 2 to 50 Hz. It is a natural decision for the SPL to launch the study of the potential of a noncesiated source in line with the one selected for Linac4 and to open up a third (noncesiated) option beside those under constant development at ISIS and SNS. The main plasma heating and beam parameters of selected H^- ion sources for accelerators are presented in Table I. The design of a 50 Hz plasma generator extrapolated from DESY's volume source is presented in this paper. The Linac4 and SPL plasma generators are shown in Fig. 1, with one half section of each source being displayed to allow a direct comparison.

II. SPL PROJECT PLASMA GENERATOR

The operation of the DESY ion source at higher rf power is being addressed on the Linac4 test stand at CERN where a 100 kW, 2 MHz rf power supply is coupled to a copy of the DESY ion source manufactured at CERN.[8] The main goal of the test is to measure the increase in H^- current resulting from a 100 kW rf injection and to demonstrate that the beam characteristics of the ion source are matching those of Linac4. For the SPL, the plasma generator will be submitted to two orders of magnitude higher duty factor than the DESY ion source. Its design is based on a thermal analysis to identify the heat fluxes; we then intend to utilize separated water

TABLE I. Plasma generator (peak power, frequency ν, and extraction voltage) and H^- pulse (pulse current, duration τ, and rms emittance ε) parameters of selected ion sources. Published experimental results are given for operational ion sources while projected values are in italic (*).

	Power rf-arc[(x)]			H^- pulse		
	P kW	ν Hz	HV kV	I mA	τ ms	ε π μm
DESY[a]	30	3	35	40	0.15	0.25
*Linac4**	*100*	*2*	*45*	*80*	*0.4*	*0.25*
*SPL**	*100*	*50*	*45*	*80*	*1.2*	*0.25*
SNS[b,c]	80	60	65	65	0.5	0.25
ISIS[d]	4^x	50	35	70	0.25	0.5

[a]Reference 1.
[b]Reference 5
[c]Reference 6.
[d]Reference 7.

[a)]Contributed paper, published as part of the Proceedings of the 13th International Conference on Ion Sources, Gatlinburg, Tennessee, September 2009.
[b)]Electronic mail: jacques.lettry@cern.ch.

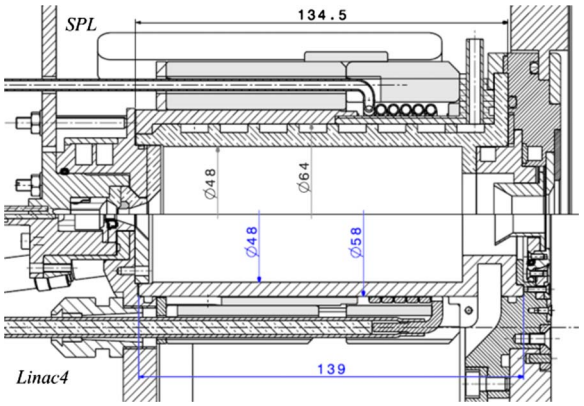

FIG. 1. (Color online) Comparing the scheme of the SPL (water cooled, top) and Linac4 (bottom) plasma generators.

cooling systems, select high thermal conductivity materials, and wherever possible, braze insulators on metals to suppress undefined low pressure contact heat barriers.

The thermal analysis of the Linac4 plasma generator is presented in Refs. 9 and 10 and the required improvements to dissipate the heat at the higher SPL duty factor are listed in Ref. 11. In Secs. II A–II D, we describe the subassembly cooling systems and underline the plasma generator features that must be preserved in order to ensure its compatibility as part of an ion source.

A. Gas injection and ignition system

The pulsed H_2-gas injection of the DESY and Linac4 ion sources rely on a piezovalve opened during a fraction of a millisecond. The burst of gas is injected into the plasma chamber via a spark-gap chamber in which a discharge with a few-ampere current is generated by a 40 μs, 600–800 V pulse. Local plasma is generated in the discharge. In Linac4, its emission light is monitored by a phototransistor. This feature is not included in the SPL plasma chamber as the emission light spectra will be recorded through the ion-extraction hole. The SPL ignition system is shown in Fig. 2, a cooling groove and Pt-100 resistors for temperature monitoring are added.

As an option, the cathode that is currently at the potential of the plasma chamber can be insulated. Setting the spark gap at a floating potential of a few hundred volts should allow the injection of electrons of defined energy into the plasma chamber. Typical timing of the gas injection, ignition, rf-pulse, and H^- production measured during the commissioning of the Linac4 ion source are shown in Fig. 3.

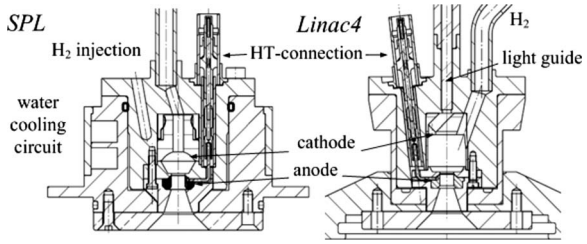

FIG. 2. Detail of the spark gap plasma ignition systems: SPL with its cooling circuit (left) and Linac4 (right).

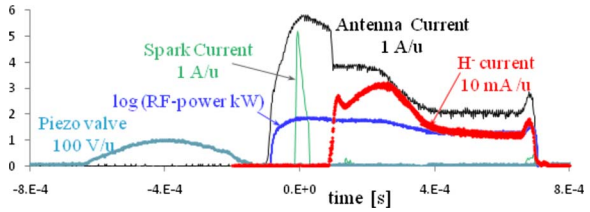

FIG. 3. (Color online) Typical timing wave forms of the gas injection, rf pulse, ignition, and H^- production measured during the commissioning of the Linac4 ion source.

The pressure-dependent delay between spark and plasma ignition may be the result of the time required for the expansion of the spark's plasma into the plasma chamber and governed by gas dynamics.

B. Plasma chamber

Heat transfer for the state of thermal equilibrium is simulated under the conservative assumption that the rf power is fully transmitted to the plasma and then transferred onto the inner wall of the plasma chamber as black-body radiation emanating from a rotational ellipsoid centered in the rf antenna. The heat radiated onto the cylindrical plasma chamber accounts for 91% of the total heat load. The first iteration showed that the alumina must be replaced by aluminum nitride and that water cooling in direct contact is mandatory. Race track, parallel, and helical cooling geometries are compared using ANSYS and their static thermal stresses assessed. A helical cooling groove machined within the AlN ceramics and covered by two cylinders (necessary for the antenna assembly) is chosen and ensures that all components of the plasma chamber are kept within material specification. The simulated flow pattern is shown in Fig. 4; the pressure drop of the helix circuit is 0.22 bar and the water temperature rises by 18° for a flow rate of 3.6 l/min. Measurement of the cooling water temperature increase and of the power dissipated in the matching circuit or reflected to the rf-power supply will improve our assessments.

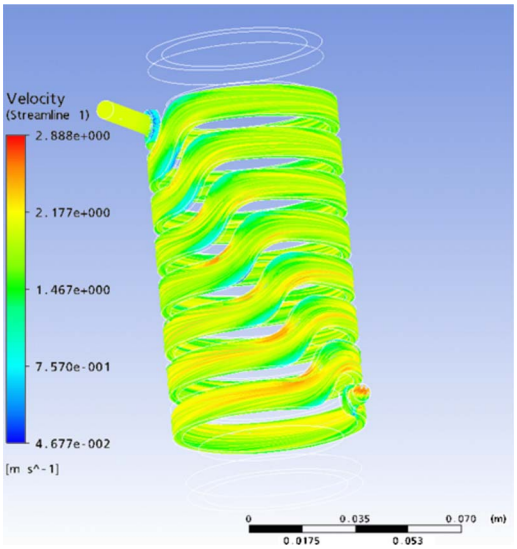

FIG. 4. (Color online) Simulation of the helical coolant flow around the plasma chamber ($v < 2.9$ m/s).

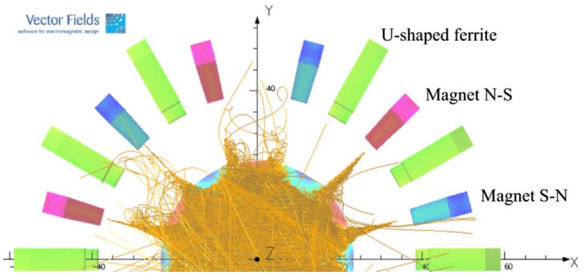

FIG. 5. (Color online) Magnetic element configuration (3D): 12 magnets and ten U-shaped ferrites. Sets of electrons were generated in the yz plane and their tracks illustrate the escape regions of the cusp confinement.

C. Magnetic confinement and antenna

The radius of the 12 permanent magnets in cusp configuration must be increased by the thickness of the plasma chamber cooling circuit. The simulation results are illustrated in Fig. 5 in order to visualize the electron confinement, a set of 5 eV electrons starting from a plane perpendicular to the plasma chamber axis is traced.

The antenna coil needs to be water cooled, a 2–4 mm insulated Cu tube is proposed. The dependence on the coil diameter of the current coupling to the plasma is compensated by leaving enough space for the coil to increase the five windings of the Linac4 source up to ten in two layers. The ten ferrites are also moved outward by the thickness of the cooling circuit. The Ni coating (20 μm) of the magnets is justified by the estimated rf induced heating of the permanent magnets and ferrites.[11]

D. H⁻ ion-extraction region

According to heat flow simulation, the extraction region composed of a filter magnet, a collar, and an extraction plate receives 8% of the heat radiated by the plasma. A dedicated cooling circuit was simulated; however, despite replacing mica and ceramics by high conductivity AlN, the presence of low pressure mechanical contacts brought the temperatures above material specifications. These thermal barriers were replaced by brazing AlN electrical insulators on the collar and extraction plate which solved this issue. The layout of the extraction region is presented in Fig. 6. Brazing tests confirmed the feasibility of this option. However, the tunable

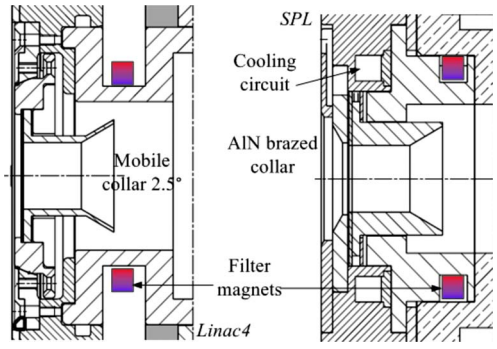

FIG. 6. (Color online) Detail of the extraction collar: Linac4 mobile collar (left) and brazed AlN insulators on the SPL collar (right). Brazing is implemented in order to reduce the thermal barrier of low pressure contacts.

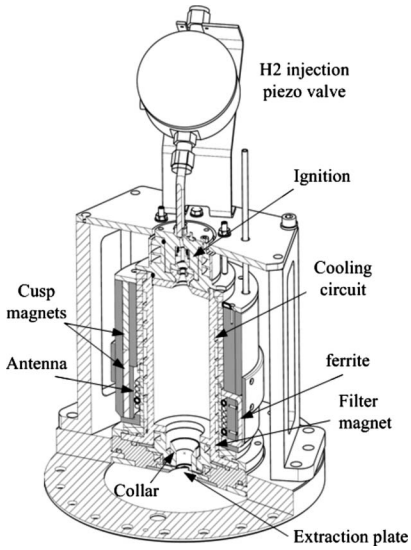

FIG. 7. 3D view of the SPL plasma generator (piezovalve, glow discharge ignition, AlN-plasma chamber, cusp magnets, ferrites, antenna, and extraction region).

front plate tilt mechanism (up to 2.5°) had to be dropped; its functionality will be either located in the ion extraction system or obtained by machining the required angle prior to brazing.

III. CONCLUSION AND OUTLOOK

The design of the SPL plasma generator is completed, a three-dimensional (3D) computer-aided design model presented in Fig. 7 is available[12] and will be used as a base for the production of a prototype that will be assembled and tested in 2010.

ACKNOWLEDGMENTS

This project has received funding from the European Community's Seventh Framework Programme (FP7/2007-2013) under Grant Agreement No. 212114.

[1] J. Peters, PAC05 Conference Proceedings, 2005 (unpublished), p. 788.
[2] D. Küchler, T. Meinschad, J. Peters, and R. Scrivens, Rev. Sci. Instrum. **79**, 02A504 (2008).
[3] L. Arnaudon *et al.*, Report No. CERN-AB-2006-084 ABP/RF, 2006.
[4] M. Baylac *et al.*, Report No. CERN-2006-006, 2006.
[5] R. F. Welton, M. P. Stockli, S. N. Murray *et al.*, AIP Conf. Proc. **1097**, 181 (2009).
[6] R. F. Welton, M. P. Stockli, S. N. Murray, T. R. Pennisi, B. Han, Y. Kang, R. H. Goulding, D. W. Crisp, D. O. Sparks, N. P. Luciano, J. R. Carmichael, and J. Carr, Rev. Sci. Instrum. **79**, 02C721 (2008).
[7] D. C. Faircloth, S. Lawrie, A. P. Letchford, C. Gabor, P. Wise, M. Whitehead, T. Wood, M. Perkins, M. Bates, P. J. Savage, D. A. Lee, and J. K. Pozimski, Rev. Sci. Instrum. **81**, 02A721 (2010).
[8] M. Kronberger, D. Küchler, J. Lettry, Ø. Midttun, M. O'Neil, M. Paoluzzi, and R. Scrivens, Rev. Sci. Instrum. **81**, 02A708 (2010).
[9] M. Kronberger, J. Lettry, and R. Scrivens, Report No. SLHC-PP-7.1.1-982420-v1.0, 2009.
[10] D. Faircloth, M. Kronberger, D. Küchler, J. Lettry, and R. Scrivens, Rev. Sci. Instrum. **81**, 02A722 (2010).
[11] M. D. Faircloth, M. Kronberger, J. Lettry, C.-M. Schmitzer, and R. Scrivens, Report No. SLHC-PP-M7.1-1002168-v1.0, 2009.
[12] M. Kronberger, E. Chaudet, D. Faircloth *et al.*, Report No. SLHC-PP-D7.1.2-1049282-v1.0, 2009.